Cavity-Based Reservoir Engineering for Floquet-Engineered Superconducting Circuits

Francesco Petiziol* and André Eckardt
Technische Universität Berlin, Institut für Theoretische Physik, Hardenbergstraße 36, Berlin 10623, Germany

(Received 3 June 2022; revised 20 September 2022; accepted 25 October 2022; published 30 November 2022)

Considering the example of superconducting circuits, we show how Floquet engineering can be combined with reservoir engineering for the controlled preparation of target states. Floquet engineering refers to the control of a quantum system by means of time-periodic forcing, typically in the high-frequency regime, so that the system is governed effectively by a time-independent Floquet Hamiltonian with novel interesting properties. Reservoir engineering, on the other hand, can be achieved in superconducting circuits by coupling a system of artificial atoms (or qubits) dispersively to pumped leaky cavities, so that the induced dissipation guides the system into a desired target state. It is not obvious that the two approaches can be combined, since reaching the dispersive regime, in which system and cavities exchange excitations only virtually, can be spoiled by driving-induced resonant transitions. However, working in the extended Floquet space and treating both system-cavity coupling as well as driving-induced excitation processes on the same footing perturbatively, we identify regimes, where reservoir engineering of targeted Floquet states is possible and accurately described by an effective time-independent master equation. We successfully benchmark our approach for the preparation of the ground state in a system of interacting bosons subjected to Floquet-engineered magnetic fields in different lattice geometries.

DOI: 10.1103/PhysRevLett.129.233601

Floquet engineering is a powerful tool for quantum simulation, where time-periodic driving is applied to manipulate the properties of a quantum system [1–6]. It has been applied successfully to engineered quantum systems, such as ultracold atoms in optical lattices [7–15], photons in optical waveguides [16–18], and superconducting circuits [19]. Recently, the question has been addressed, whether it is possible to prepare ground (or low-temperature) states of effective Floquet-engineered Hamiltonians by coupling them to a thermal environment [20–26]. Here we propose an alternative strategy for dissipative state preparation in Floquet systems based on cavity-assisted reservoir engineering, as it can be realized in superconducting circuits by coupling artificial atoms to pumped leaky resonators. Such an approach is not straightforward, since cavity-based reservoir engineering relies on the so-called dispersive regime, in which the system exchanges excitations with the cavities only virtually. Thus, one has to identify a regime, in which such a virtual change is not spoiled by driving-induced resonant processes. Understanding and avoiding the breakdown of dispersive regimes in circuit QED systems under periodic modulation is a central challenge, as investigated, e.g., in the realization of fast gates and controlled nonlinearities for high-Q cavity modes coupled via driven transmons [27,28]. To solve this problem, we describe both atoms and cavities in the extended Floquet space. In this framework, we treat both the system-bath coupling as well as driving-induced excitation processes on equal footing using degenerate perturbation theory. This combined approach contains both the standard perturbative treatment of the dispersive coupling in nondriven systems as well as the high-frequency expansion of isolated periodically driven systems as limiting cases. But it also includes the interplay of both processes, which has a crucial (potentially detrimental) impact on the open driven dynamics and the preparation of target states. Based on this theory, we formulate driven-dissipative schemes for the preparation of nontrivial states in finite Floquet-engineered flux ladders (exhibiting chiral ground state currents and frustration-induced localization effects). The approach is confirmed via simulations of the full driven-dissipative evolution of atoms and cavities.

We consider a two-dimensional array of M artificial atoms (Fig. 1) in a superconducting circuit [19,29–32] described by the Bose-Hubbard Hamiltonian

$$\hat{H}_S(t) = \frac{U}{2}\sum_{j=1}^{M}\hat{n}_j(\hat{n}_j-1) - J\sum_{\langle j,j'\rangle} e^{i\theta_{j'j}(t)}\hat{a}_{j'}^{\dagger}\hat{a}_j. \quad (1)$$

Here $\hat{a}_j$ and $\hat{n}_j = \hat{a}_j^{\dagger}\hat{a}_j$ denote the bosonic annihilation and number operators for an excitation on site j. The excitations experience an attractive on site potential $U < 0$, corresponding to a level anharmonicity. Moreover, they can tunnel between neighboring sites with matrix elements of amplitude $J > 0$. The time-periodic Peierls phases $\theta_{ij}(t) = \theta_i(t) - \theta_j(t)$ describe a time-dependent force, which, in a nonrotating reference frame, is described by on site potentials $v_j = \hbar\dot{\theta}_j = \Delta + \nu_j\hbar\omega + \lambda\sin(\omega t - \varphi_j)$ with integer ν_j. The transition to the rotating frame adopted in Eq. (1)

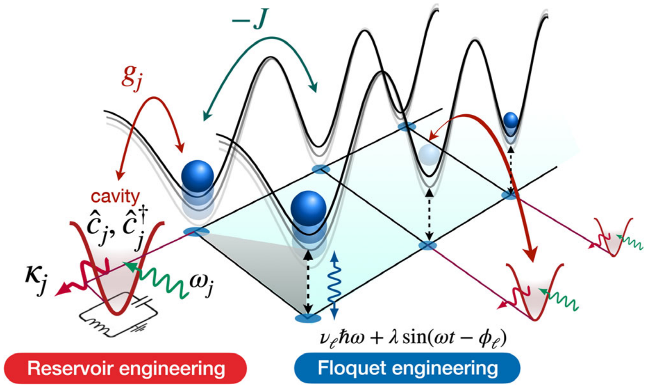

FIG. 1. M artificial atoms are coupled to L pumped and leaky cavities. The atoms are periodically driven to Floquet engineer effective Hamiltonians with desired properties, while the cavities induce dissipation in a controlled way.

and considered in the following, is accomplished by replacing $\hat{a}_j \to e^{-i\theta_j(t)}\hat{a}_j$ with $\theta_j(t) = \Delta t/\hbar + \nu_j \omega t - \lambda \cos(\omega t - \varphi_j)/\hbar\omega$.

For isolated systems, the motivation for applying such periodic forcing is that in the high-frequency regime, $\hbar\omega \gg |U|, J$ the dynamics is approximately described by an effective time-independent Hamiltonian $\hat{H}_S^{\rm eff}$, with new properties. In leading order, it is obtained as time average $\hat{H}_S^{\rm eff} = (1/T)\int_0^T dt \hat{H}_S(t)$ over one driving period $T = 2\pi/\omega$ (rotating-wave approximation). This gives rise to effective tunneling matrix elements $-J_{jj'}^{\rm eff} e^{i\theta_{jj'}^{\rm eff}}$, with amplitude $J_{jj'}^{\rm eff} = J\mathcal{J}_{\nu_j-\nu_{j'}}(2\lambda \sin[(\varphi_{j'} - \varphi_j)/2]/\hbar\omega)$, where $\mathcal{J}_n(\cdot)$ denotes a Bessel function, and with Peierls phases $\theta_{jj'}^{\rm eff} = (\nu_{j'} - \nu_j)(\varphi_j + \varphi_{j'})/2$, which can describe artificial magnetic fields [3]. Such (and similar) Floquet engineering has been employed successfully to experimentally engineer and study interaction-driven phase transitions [8], kinetic frustration [9], topological band structures [11,12,15], their chiral edge modes [16,17,19], Aharonov-Bohm cages [33], and 2-qubit gates [32,34] in systems of ultracold atoms in optical lattices, optical waveguides, and superconducting circuits.

We will investigate, whether it is possible to employ reservoir engineering for cooling the system into the ground state of $\hat{H}_S^{\rm eff}$. To this end, some of the atoms shall be coupled individually to driven-damped cavities. The open dynamics of the whole system is described by the master equation $d\hat{\rho}/dt = -i[\hat{H}(t), \hat{\rho}]/\hbar + \sum_{\ell=1}^{L} \kappa_\ell \mathcal{D}[\hat{c}_\ell]\hat{\rho}$, where $\mathcal{D}[\hat{c}_\ell]\hat{\rho} = \hat{c}_\ell \hat{\rho} \hat{c}_\ell^\dagger - \frac{1}{2}\hat{c}_\ell^\dagger \hat{c}_\ell \hat{\rho} - \frac{1}{2}\hat{\rho}\hat{c}_\ell^\dagger \hat{c}_\ell$ is a Lindblad dissipator and where the Hamiltonian $\hat{H}(t) = \hat{H}_S(t) + \hat{H}_{SC}(t) + \hat{H}_C(t)$ comprises the terms $\hat{H}_C(t) = \sum_{j=1}^{L}[\delta_j \hat{c}_j^\dagger \hat{c}_j + \mathcal{E}_j \hat{c}_j^\dagger e^{-i\omega_j t} + \mathcal{E}_j^* \hat{c}_j e^{i\omega_j t}]$ and $\hat{H}_{SC}(t) = \sum_{j=1}^{L} g_j[e^{-i\theta_j(t)}\hat{a}_j \hat{c}_j^\dagger + \text{H.c.}]$ that describe the cavities in a frame rotating at frequency $\Delta/\hbar$ and their coupling to the system [32,35]. The $L \le M$ cavities are described by bosonic annihilation operators $\hat{c}_j$, are detuned by the atoms by δ_j, pumped with strength $\mathcal{E}_j$ at a frequency ω_j, and leak photons at a rate κ_j. The atoms are enumerated so that the jth cavity couples to the jth atom with strength g_j. The cavity leakage is assumed to be much larger than other decay and dephasing rates in the array, which we thus neglect in the following. The Floquet drive also dresses the array-cavity tunnelling, which hence acquires the phase $\theta_j(t)$.

The atom-cavity Hamiltonian $\hat{H}(t) \equiv \sum_m \hat{H}_m e^{im\omega t}$ gives rise to Floquet states $|\psi_n(t)\rangle = |u_n(t)\rangle e^{-i\varepsilon_n t/\hbar} = |u_{n\mu}(t)\rangle e^{-i\varepsilon_{n\mu} t/\hbar}$ with quasienergies $\varepsilon_{n\mu} = \varepsilon_n + \mu\hbar\omega$ that are defined up to integer multiples μ of $\hbar\omega$ and time-periodic Floquet modes $|u_{n\mu}(t)\rangle = |u_n(t)\rangle e^{i\mu\omega t} = |u_{n\mu}(t+T)\rangle \equiv \sum_{\boldsymbol{n},\boldsymbol{p},m} u_{n\mu}^{(\boldsymbol{np}m)} |\boldsymbol{np}\rangle e^{im\omega t}$. Here $|\boldsymbol{np}\rangle$ denote Fock states with respect to the occupation numbers $\boldsymbol{n} = (n_1, \ldots, n_M)$ of system excitations and $\boldsymbol{p} = (p_1, \ldots, p_L)$ of cavity photons, and m is an integer Fourier index. In Floquet space [3,36], spanned by the Floquet-Fock states $|\boldsymbol{np}m\rangle\rangle$ (representing $|\boldsymbol{np}\rangle e^{im\omega t}$ in the original space), the Floquet modes $|u_{n\mu}\rangle\rangle = \sum_{\boldsymbol{n},\boldsymbol{p},m} u_{n\mu}^{(\boldsymbol{np}m)} |\boldsymbol{np}m\rangle\rangle$ are eigenstates with eigenvalue $\varepsilon_{n\mu}$ of the generalized Hamiltonian $\hat{\mathcal{H}}$ [representing $\hat{H}(t) - i\hbar\partial_t$] with matrix elements

$$\langle\langle \boldsymbol{n}'\boldsymbol{p}'m'|\hat{\mathcal{H}}|\boldsymbol{np}m\rangle\rangle = \langle \boldsymbol{n}'\boldsymbol{p}'|(\hat{H}_{m'-m} + \delta_{m'm} m\hbar\omega)|\boldsymbol{np}\rangle. \quad (2)$$

The change of m by $\Delta m = m' - m \neq 0$, as it is described by the Fourier components $\hat{H}_{\Delta m}$, corresponds to a resonant transition, where the energy changes by Δm driving quanta $\hbar\omega$. In turn, processes without such driving-induced energy change are captured by the time-averaged Hamiltonian $\hat{H}_{\Delta m=0}$, which contains $\hat{H}_S^{\rm eff}$.

For Floquet engineering, we aim at a regime, where m remains a good quantum number, such that the array coherent dynamics is indeed ruled by $\hat{H}_S^{\rm eff}$. For reservoir engineering, we aim at a regime, where the total excitation number N remains a good quantum number, since we strive for quantum simulation at a conserved particle number. We, thus, aim at a situation, where energy and excitation-number-changing processes can be treated using degenerate perturbation theory, allowing us to block diagonalize $\hat{\mathcal{H}}$ both with respect to m and N. This is challenging. While resonances, where m or N change individually are routinely suppressed by making the associated energy costs, the frequency $\hbar\omega$ or the atom-cavity detuning δ_j, respectively, large, it is now also required to avoid resonances where both m and N change. Similar processes are sketched in Figs. 2(a) and 2(b), where an excitation can escape [(a)] or be injected [(b)] in the array by exchanging energy $m\hbar\omega$ with the Floquet drive. Although for a weak transverse single-qubit drive as in Ref. [37] these are very high-order processes, they strongly challenge usual dispersive-regime

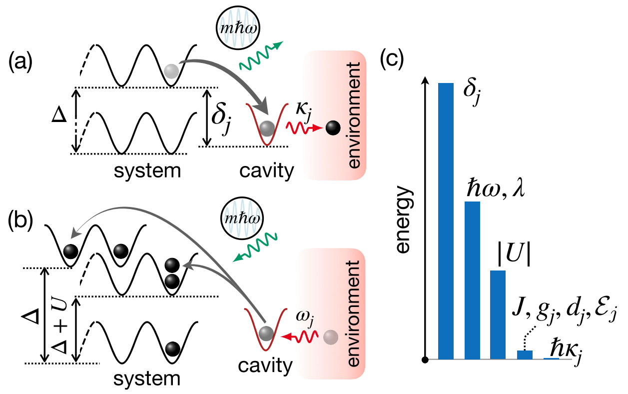

FIG. 2. (a) and (b) Examples of unwanted excitation-photon conversion assisted by the Floquet drive. In (a), an excitation tunnels from the array to a cavity releasing an energy $m\hbar\omega$ to the drive, and leaks to the environment being lost. In (b), a photon tunnels from the cavity to the array. (c) Fundamental energy scales in the system.

treatments here and cannot be neglected. Nonetheless, as we will see, the desired regime can be found.

A suitable description is achieved by performing a two-step block-diagonalization of $\hat{\mathcal{H}}$ using van Vleck-type degenerate perturbation theory in Floquet space [38,39]. This approach captures corrections arising from processes changing both m and N in second order (except for second-order processes with respect to m alone, which would yield the first correction of $\hat{H}_S^{\rm eff}$ in a high-frequency expansion and are not relevant here). Such mixed processes would be discarded when time averaging the total Hamiltonian before or after having performed a dispersive-regime transformation, as it is done in Ref. [37]. This makes our approach decisive for obtaining correct effective parameters both for the coherent and incoherent dynamics, as confirmed by numerical simulations. We arrive at the effective atom-cavity Hamiltonian [39]

$$\hat{H}_{\rm eff} = \hat{H}_S^{\rm eff} + \hat{H}_C + \sum_{j=1}^{L} [\xi_j(\hat{n}_j - 1)\hat{n}_j + \chi_j(\hat{n}_j)\hat{c}_j^\dagger \hat{c}_j], \quad (3)$$

with functions $\chi_j(\hat{n}_j) = \tilde{\chi}_j(\hat{n}_j) - \xi_j(\hat{n}_j)$ and

$$\tilde{\chi}_j(\hat{n}_j) = \sum_{m=-\infty}^{+\infty} \frac{g_j^2 U \mathcal{J}_m^2(\lambda/\hbar\omega)\hat{n}_j}{[\delta_j + U(\hat{n}_j - 1) - m\hbar\omega][\delta_j + U\hat{n}_j - m\hbar\omega]},$$
$$\xi_j(\hat{n}_j) = \sum_{m=-\infty}^{+\infty} \frac{g_j^2 \mathcal{J}_m^2(\lambda/\hbar\omega)}{\delta_j + U\hat{n}_j - m\hbar\omega}. \quad (4)$$

The coupling to the cavities in Eq. (3) involves only operators preserving the total number of atomic excitations. The prominent role played by the Floquet drive is reflected in the effective tunnelling rate and atom-cavity coupling, which explicitly depend on the driving frequency ω and amplitude λ. Equation (3) can only be valid as long as resonances are avoided that make the denominators of Eq. (4) small. A sketch of the relation between different energy scales in the system, that permit the approximations adopted while being experimentally realistic, is shown in Fig. 2(c). The starting point is the dispersive regime, where $|\delta_j| \gg g_j$, with a strong nonlinearity $|U| \gg g_j$ that enhances the virtual coupling; see Eq. (4). Next $\hbar\omega, \lambda \gg J, g_j$ is chosen to enable Floquet engineering of the tunnelling dynamics, while avoiding resonances.

Applying the perturbative treatment to the full master equation [39,45], an effective dissipator $\mathcal{D}_{\rm eff}(\hat{\rho})$ is obtained, $\mathcal{D}_{\rm eff}(\hat{\rho}) = \sum_{j=1}^{L} \kappa_j \sum_{m=-\infty}^{+\infty} \mathcal{D}[\hat{c}_{j,m}](\hat{\rho})$, with

$$\hat{c}_{j,m} = \hat{c}_j \delta_{m,0} + \frac{g_j \mathcal{J}_m(\lambda/\hbar\omega)}{\delta_j + U\hat{n}_j - m\hbar\omega} \hat{a}_j. \quad (5)$$

Since the block diagonalization of $\hat{\mathcal{H}}$ mixes atom and cavity degrees of freedom, $\mathcal{D}_{\rm eff}(\hat{\rho})$ does not involve cavity decay only, but also a small perturbative term $\propto \hat{a}_j$, describing excitation loss from the system. This is analogous to the undriven case in the dispersive regime [32], except for additional driving-induced decay channels with $m \neq 0$. The excitation loss is weak in the perturbative regime assumed here, and can be counteracted by postselection [39]. In a proof-of-principle implementation, where state tomography in the relevant subspace is accessible, this can be done directly from the estimated density matrix. In large systems, we consider observables that, while being key signatures of the desired effects, also carry information about the total excitation number allowing for postselection. These are site occupations and excitation currents. The former are extracted directly by dispersive readout of the atomic excitations; the latter can be detected as done in cold atom experiments [11,46], by biasing the on site potentials $v_j(t)$ of pairs of neighboring sites (which is an excitation-conserving process) and measuring the time evolution of site occupations.

The form of the array-cavity coupling in $\hat{H}_{\rm eff}$ puts us in a position, where reservoir engineering for the atoms can be realized. The underlying mechanism is that incoming pump photons that are detuned from the cavity resonance, need to take (or give) energy from (to) the system, before being emitted at the cavity frequency [35,37,47]. If the detuning matches an energy gap in the atomic system, this induces a corresponding "dissipative" transition. This type of quantum bath engineering has been implemented experimentally with superconducting circuits, e.g., for a resonantly driven two-level system and for a three-site undriven Bose-Hubbard chain [35,37]. In our setup, since the relevant atomic Hamiltonian is the Floquet-engineered Hamiltonian $\hat{H}_S^{\rm eff}$, we exploit this mechanism to address transitions among effective eigenstates of the system with artificial magnetic flux.

To design a dissipative path, driving the atoms toward a target eigenstate of $\hat{H}_S^{\rm eff} = \sum_\eta \varepsilon_\eta |\eta\rangle\langle\eta|$, the cavity-pump detunings d_j are set to match different effective energy gaps $\varepsilon_\eta - \varepsilon_{\eta'}$ in the array. Addressing single gaps is possible provided such gaps are larger than the effective atom-cavity coupling $\chi_j^{(\eta\eta')}\sqrt{\bar{n}_{{\rm ph},j}}$, where $\bar{n}_{{\rm ph},j}$ is the mean photon number in the jth cavity and $\chi_j^{(\eta\eta')} = \langle\eta|\chi_j(\hat{n}_j))|\eta'\rangle$ is the matrix element of the atomic coupling operator. The resonant transition rate produced by the jth cavity is derived from the effective master equation [39] as

$$\Gamma^{(j)}_{\eta\to\eta'} = 4\bar{n}_{{\rm ph},j}|\chi_j^{(\eta\eta')}|^2/\hbar^2\kappa_j, \qquad (6)$$

under the "bad-cavity" condition that the photon leakage is strong compared with the effective coupling, $\hbar\kappa_j \gg \chi_j^{(\eta\eta')}\sqrt{\bar{n}_{{\rm ph},j}}$. This condition guarantees a clean monotonic exponential decay from $|\eta\rangle$ to $|\eta'\rangle$, but is not strictly essential: a smaller κ_j can still achieve the desired transition, though producing more complex decay dynamics due to the atom-cavity system reaching an effective strong-coupling regime [37].

We test the proposed scheme for different systems with Floquet-engineered artificial fluxes. We will compare our effective theory to a full simulation of the time-dependent master equation for both system and cavities, using typical circuit-QED parameters. Given the latter, the determination of the parameters ensuring a successful protocol can be done systematically: while $\hbar\omega$ and the shift Δ are chosen to be much larger than J and fine-tuned to avoid unwanted resonances, the pump frequencies on the cavities realize the detuning conditions for reservoir engineering. The pump amplitudes are adjusted accordingly to have an average number of one-to-two photons in the cavities, which gave best results in simulations. Further details on parameter choices are given in Ref. [39].

We start by considering one excitation in a ladder-type array [Fig. 3(a)]. The ground state for nonzero magnetic flux Φ can exhibit chiral currents, flowing unidirectionally along the edges of the ladder [11,48–51]. Although only one excitation is considered, including subspaces with several excitations and their mutual interactions U is essential, since it influences virtual excitation-number fluctuations exploited for reservoir engineering; see Eqs. (3) and (4). In the two-plaquette system of Fig. 3(a), the ground state is prepared using two cavities which realize a "cascaded" cooling configuration along the effective spectrum as depicted in Fig. 3(b) (left). The driving amplitude λ is chosen to give the same effective tunnelling rate $J_{\rm eff}$ along every lattice bond, while the choice of driving phases and potential offsets yields Peierls phases $r\Phi$ at the rth rung [39]. The simulated buildup of population in the ground

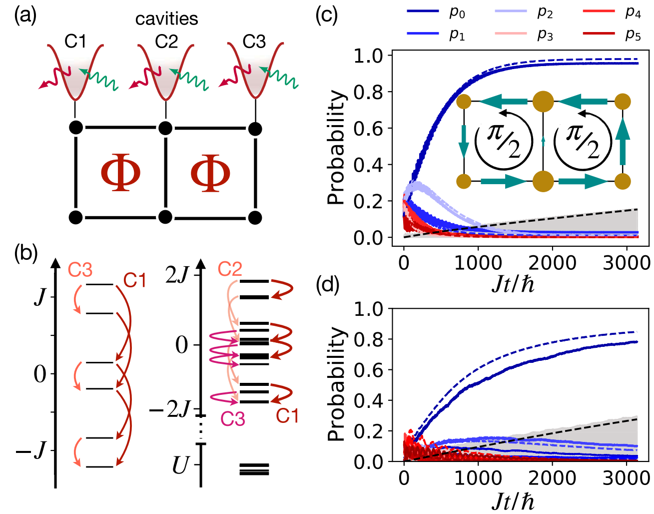

FIG. 3. (a) Ladder geometry and coupling to the cavities. (b) Single-excitation (left) and two-excitation (right) level structure and transition energies addressed by the cavities (arrows). (c) Stroboscopic evolution of the populations $p_\eta(t) = \langle\eta|\hat{\rho}(t)|\eta\rangle$ of the eigenstates $|\eta\rangle$ of $\hat{H}_S^{\rm eff}$, for the full driven master equation (solid) and the effective master equation (dashed). The gray shaded area indicates the fraction of discarded states in postselection (black dashed line for the effective model). The parameters are $\Phi = \pi/2$, $\hbar\omega = 20J$, $\boldsymbol{\delta}/\hbar\omega = (1.76, 1.7)$, $U = 8J$, $\kappa_1 = \kappa_2 = 0.1J$, $\boldsymbol{\mathcal{E}}/J = (1.2, 0.5)$, $g_1 = g_2 = J$. Inset: The size of the arrows and circles reproduces the current pattern and excitation density in the final state. (d) As (c) but for two excitations in the hard-core bosons subspace. The parameters are $\Phi = \pi/2$, $\hbar\omega = 20J$, $\boldsymbol{\delta}/\hbar\omega = (1.69, 1.68, 1.7)$, $U = 8J$, $\boldsymbol{\kappa}/J = (0.05, 0.05, 0.05)$, $\boldsymbol{\mathcal{E}}/J = (0.6, 1.6, 0.4)$, $\boldsymbol{g}/J = (1, 1, 1)$.

state in time is shown in Fig. 3(c), leading to the final current and density pattern depicted in the inset. The cooling is independent from the initial state. While in Fig. 3(c) the initial state features the excitation sitting in one atom, an equivalent population buildup is also observed for mixed initial states, such as an infinite-temperature state in the single-excitation manifold. This confirms that the cooling mechanism can reduce the system entropy, in addition to lowering the energy. A cooling scheme in the case of a three-plaquette ladder is reported in Ref. [39].

The protocol is also effective for multiple excitations. When a second excitation is injected, due to the large on site interaction U, singly and doubly excited atoms define two essentially uncoupled subspaces [Fig. 3(b), right], corresponding to hard-core bosons and a tightly bound pair, respectively. The former subspace is most interesting [as, for instance, hard-core bosons in finite two-dimensional lattices with homogeneous flux are predicted to give rise to fractional-quantum-Hall (FQH)-type ground states [52–54]], and we can use three cavities to cool the system into the hard-core-boson ground state. Starting with two excitations localized in different sites, achievable by exciting two atoms to state $a^\dagger_{j'}a^\dagger_j|0\rangle$ with quick resonant

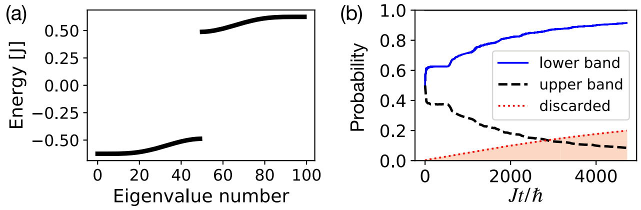

FIG. 4. (a) Bands in a 100 sites ladder and (b) interband cooling of one excitation using two cavities. Parameters $\Phi = 0.8\pi$, $\hbar\omega = 20J$, $\lambda \simeq 1.16\hbar\omega$, $d_1 = d_2 = J$, $\delta_1 = \delta_2 = 34.4J$, $g_1 = g_2 = J$, $\mathcal{E}_1 = \mathcal{E}_2 = 1.4J$. The shaded region indicates the fraction of discarded records in postselection.

pulses before launching the Floquet drives, the population buildup in time is shown in Fig. 3(d).

From Figs. 3(c) and 3(d), one can see that the effective master equation reproduces the results of the full model very accurately, that the fraction of discarded data in postselection remains small and does not render the experiment inefficient, and that the target states can be prepared with rather high fidelities. In the Supplemental Material [39], we discuss the geometry of a diamond-chain of corner-sharing rhombic plaquettes with flux $\Phi = \pi$ and the preparation of so-called Aharonov Bohm cages—single-excitation states that are localized in a subsystem via destructive interference [33,55,56].

Until now we have addressed the preparation of (zero-temperature) ground states in systems of moderate size. The essential ingredients demonstrated in these examples also provide a perspective for potential applications in larger systems. Namely, the preparation of a gapped ground state, like a Floquet-engineered (topological) band insulator or a correlated fractional Chern insulator, appear possible. Although for a large system, the number of cavities cannot scale as quickly as the number of transitions, multiple transitions can be controlled with a single cavity when they lie in an energy window comparable with the cavity linewidth $\hbar\kappa$ [39]. This effect can already be appreciated from the two-excitation example of Figs. 3(b)–3(d), where three cavities only are enough to work effectively in the two-excitation subspace (21 states). Another issue with large systems is resonant excitations. Namely the gapped state will most likely be embedded into a continuum of excited states to which it couples resonantly. Although this might limit the capability to resolve the exact ground state, playing a role similar to an effective nonzero temperature, the preparation of low-energy and low-entropy states can still be addressed.

We further exemplify the control of multiple transitions in a larger system, by considering a 100-site square ladder with flux $\Phi = 0.8\pi$ and tunnelling along the rungs five times faster than along the legs, whose effective spectrum features two well separated narrow bands [Fig. 4(a)]. One excitation initialized at a site overlaps with all states in both bands, but can be dissipatively pushed into the lower band using two cavities only, coupled to the two ends of the upper leg. We demonstrate this successfully by performing simulations with the effective master equation [Fig. 4(b)]. This example further highlights that Floquet-dissipative schemes can also be used to project a system into a (quasi) energetically well separated subspace, opening potential applications for autonomous quantum error correction [57,58] and the preparation of gapped ground states (such as FQH states [52–54,59]). In view of the latter, particularly exciting is the combination of artificial gauge fields [1,4] or geometric frustration [9,60], as it can be achieved using Floquet engineering, with an interaction-induced hard-core constraint. Such hard-core interactions can not only be used to mimic fermionic behavior in 1D, but are also predicted to stabilize fractional-Chern-insulator states in topologically nontrivial lattice systems as well as spin-liquid-like states. Finally, the theory developed here can also find straightforward application in different platforms where Floquet engineering has been employed, such as quantum gas microscopes, whenever coupling to driven cavitylike modes is possible.

This research was funded by the German Research Foundation (DFG) via the Collaborative Research Center (SFB) 910, under Project No. 163436311, and the Research Unit FOR 2414, under Project No. 277974659.

*f.petiziol@tu-berlin.de

[1] N. Goldman and J. Dalibard, Periodically Driven Quantum Systems: Effective Hamiltonians and Engineered Gauge Fields, Phys. Rev. X **4**, 031027 (2014).
[2] M. Bukov, L. D'Alessio, and A. Polkovnikov, Universal high-frequency behavior of periodically driven systems: From dynamical stabilization to Floquet engineering, Adv. Phys. **64**, 139 (2015).
[3] A. Eckardt, Colloquium: Atomic quantum gases in periodically driven optical lattices, Rev. Mod. Phys. **89**, 011004 (2017).
[4] M. Aidelsburger, S. Nascimbene, and N. Goldman, Artificial gauge fields in materials and engineered systems, C. R. Phys. **19**, 394 (2018).
[5] T. Oka and S. Kitamura, Floquet engineering of quantum materials, Annu. Rev. Condens. Matter Phys. **10**, 387 (2019).
[6] M. S. Rudner and N. H. Lindner, Band structure engineering and non-equilibrium dynamics in Floquet topological insulators, Nat. Rev. Phys. **2**, 229 (2020).
[7] H. Lignier, C. Sias, D. Ciampini, Y. Singh, A. Zenesini, O. Morsch, and E. Arimondo, Dynamical Control of Matter-Wave Tunneling in Periodic Potentials, Phys. Rev. Lett. **99**, 220403 (2007).
[8] A. Zenesini, H. Lignier, D. Ciampini, O. Morsch, and E. Arimondo, Coherent Control of Dressed Matter Waves, Phys. Rev. Lett. **102**, 100403 (2009).
[9] J. Struck, C. lschlger, R. L. Targat, P. Soltan-Panahi, A. Eckardt, M. Lewenstein, P. Windpassinger, and K. Sengstock, Quantum simulation of frustrated classical

magnetism in triangular optical lattices, Science **333**, 996 (2011).

[10] J. Struck, C. Ölschläger, M. Weinberg, P. Hauke, J. Simonet, A. Eckardt, M. Lewenstein, K. Sengstock, and P. Windpassinger, Tunable Gauge Potential for Neutral and Spinless Particles in Driven Optical Lattices, Phys. Rev. Lett. **108**, 225304 (2012).

[11] M. Atala, M. Aidelsburger, M. Lohse, J. T. Barreiro, B. Paredes, and I. Bloch, Observation of chiral currents with ultracold atoms in bosonic ladders, Nat. Phys. **10**, 588 (2014).

[12] G. Jotzu, M. Messer, R. Desbuquois, M. Lebrat, T. Uehlinger, D. Greif, and T. Esslinger, Experimental realization of the topological Haldane model with ultracold fermions, Nature (London) **515**, 237 (2014).

[13] M. Aidelsburger, M. Lohse, C. Schweizer, M. Atala, J. T. Barreiro, S. Nascimbne, N. R. Cooper, I. Bloch, and N. Goldman, Measuring the Chern number of Hofstadter bands with ultracold bosonic atoms, Nat. Phys. **11**, 162 (2015).

[14] M. E. Tai, A. Lukin, M. Rispoli, R. S. A. Menke, D. Borgnia, P. M. Preiss, F. Grusdt, A. M. Kaufman, and M. Greiner, Microscopy of the interacting Harper-Hofstadter model in the two-body limit, Nature (London) **546**, 519 (2017).

[15] K. Wintersperger, C. Braun, F. N. Ünal, A. Eckardt, M. Di Liberto, N. Goldman, I. Bloch, and M. Aidelsburger, Realization of an anomalous Floquet topological system with ultracold atoms, Nat. Phys. **16**, 1058 (2020).

[16] M. C. Rechtsman, J. M. Zeuner, Y. Plotnik, Y. Lumer, D. Podolsky, F. Dreisow, S. Nolte, M. Segev, and A. Szameit, Photonic Floquet topological insulators, Nature (London) **496**, 196 (2013).

[17] L. J. Maczewsky, J. M. Zeuner, S. Nolte, and A. Szameit, Observation of photonic anomalous Floquet topological insulators, Nat. Commun. **8**, 13756 (2017).

[18] T. Ozawa, H. M. Price, A. Amo, N. Goldman, M. Hafezi, L. Lu, M. C. Rechtsman, D. Schuster, J. Simon, O. Zilberberg, and I. Carusotto, Topological photonics, Rev. Mod. Phys. **91**, 015006 (2019).

[19] P. Roushan *et al.*, Chiral ground-state currents of interacting photons in a synthetic magnetic field, Nat. Phys. **13**, 146 (2017).

[20] H. Breuer and M. Holthaus, A semiclassical theory of quasienergies and Floquet wave functions, Ann. Phys. (N.Y.) **211**, 249 (1991).

[21] R. Ketzmerick and W. Wustmann, Statistical mechanics of Floquet systems with regular and chaotic states, Phys. Rev. E **82**, 021114 (2010).

[22] T. Shirai, T. Mori, and S. Miyashita, Condition for emergence of the Floquet-Gibbs state in periodically driven open systems, Phys. Rev. E **91**, 030101(R) (2015).

[23] T. Shirai, J. Thingna, T. Mori, S. Denisov, P. Hnggi, and S. Miyashita, Effective Floquet–Gibbs states for dissipative quantum systems, New J. Phys. **18**, 053008 (2016).

[24] T. Mori, Floquet states in open quantum systems, arXiv:2203.16358.

[25] K. I. Seetharam, C.-E. Bardyn, N. H. Lindner, M. S. Rudner, and G. Refael, Controlled Population of Floquet-Bloch States via Coupling to Bose and Fermi Baths, Phys. Rev. X **5**, 041050 (2015).

[26] T. Iadecola, T. Neupert, and C. Chamon, Occupation of topological Floquet bands in open systems, Phys. Rev. B **91**, 235133 (2015).

[27] Y. Zhang, B. J. Lester, Y. Y. Gao, L. Jiang, R. J. Schoelkopf, and S. M. Girvin, Engineering bilinear mode coupling in circuit QED: Theory and experiment, Phys. Rev. A **99**, 012314 (2019).

[28] Y. Zhang, J. C. Curtis, C. S. Wang, R. J. Schoelkopf, and S. M. Girvin, Drive-induced nonlinearities of cavity modes coupled to a transmon ancilla, Phys. Rev. A **105**, 022423 (2022).

[29] P. Roushan *et al.*, Spectroscopic signatures of localization with interacting photons in superconducting qubits, Science **358**, 1175 (2017).

[30] R. Ma, B. Saxberg, C. Owens, N. Leung, Y. Lu, J. Simon, and D. I. Schuster, A dissipatively stabilized Mott insulator of photons, Nature (London) **566**, 51 (2019).

[31] Z. Yan *et al.*, Strongly correlated quantum walks with a 12-qubit superconducting processor, Science **364**, 753 (2019).

[32] A. Blais, A. L. Grimsmo, S. M. Girvin, and A. Wallraff, Circuit quantum electrodynamics, Rev. Mod. Phys. **93**, 025005 (2021).

[33] S. Mukherjee, M. Di Liberto, P. Öhberg, R. R. Thomson, and N. Goldman, Experimental Observation of Aharonov-Bohm Cages in Photonic Lattices, Phys. Rev. Lett. **121**, 075502 (2018).

[34] J. D. Strand, M. Ware, F. Beaudoin, T. A. Ohki, B. R. Johnson, A. Blais, and B. L. T. Plourde, First-order sideband transitions with flux-driven asymmetric transmon qubits, Phys. Rev. B **87**, 220505(R) (2013).

[35] S. Hacohen-Gourgy, V. V. Ramasesh, C. De Grandi, I. Siddiqi, and S. M. Girvin, Cooling and Autonomous Feedback in a Bose-Hubbard Chain with Attractive Interactions, Phys. Rev. Lett. **115**, 240501 (2015).

[36] H. Sambe, Steady states and quasienergies of a quantum-mechanical system in an oscillating field, Phys. Rev. A **7**, 2203 (1973).

[37] K. W. Murch, U. Vool, D. Zhou, S. J. Weber, S. M. Girvin, and I. Siddiqi, Cavity-Assisted Quantum Bath Engineering, Phys. Rev. Lett. **109**, 183602 (2012).

[38] A. Eckardt and E. Anisimovas, High-frequency approximation for periodically driven quantum systems from a Floquet-space perspective, New J. Phys. **17**, 093039 (2015).

[39] See Supplemental Material at http://link.aps.org/supplemental/10.1103/PhysRevLett.129.233601 which includes Refs. [40–44], for (i) the derivation of the effective Hamiltonian and master equation, with related driving schemes used; (ii) supplemental details on the derivation of the dissipative transition rates attained by reservoir engineering; (iii) details about numerical simulations and postselection, and the preparation of localized states; (iv) supplemental details on the choice of parameters and an illustrative example of protocol design for Floquet-dissipative state preparation.

[40] I. Shavitt and L. T. Redmon, Quasidegenerate perturbation theories. A canonical van Vleck formalism and its relationship to other approaches, J. Chem. Phys. **73**, 5711 (1980).

[41] M. O. Scully and M. S. Zubairy, *Quantum Optics, Chap. IV, Sec. 9.5* (Cambridge University Press, Cambridge, UK, 1997).

[42] K. Mølmer, Y. Castin, and J. Dalibard, Monte carlo wave-function method in quantum optics, J. Opt. Soc. Am. B **10**, 524 (1993).

[43] J. Johansson, P. Nation, and F. Nori, QuTiP: An open-source Python framework for the dynamics of open quantum systems, Comput. Phys. Commun. **183**, 1760 (2012).

[44] J. Johansson, P. Nation, and F. Nori, QuTiP 2: A Python framework for the dynamics of open quantum systems, Comput. Phys. Commun. **184**, 1234 (2013).

[45] A. Schnell, S. Denisov, and A. Eckardt, High-frequency expansions for time-periodic Lindblad generators, Phys. Rev. B **104**, 165414 (2021).

[46] S. Keßler and F. Marquardt, Single-site-resolved measurement of the current statistics in optical lattices, Phys. Rev. A **89**, 061601(R) (2014).

[47] A. A. Clerk, M. H. Devoret, S. M. Girvin, F. Marquardt, and R. J. Schoelkopf, Introduction to quantum noise, measurement, and amplification, Rev. Mod. Phys. **82**, 1155 (2010).

[48] D. Hügel and B. Paredes, Chiral ladders and the edges of quantum Hall insulators, Phys. Rev. A **89**, 023619 (2014).

[49] M. Piraud, F. Heidrich-Meisner, I. P. McCulloch, S. Greschner, T. Vekua, and U. Schollwöck, Vortex and Meissner phases of strongly interacting bosons on a two-leg ladder, Phys. Rev. B **91**, 140406(R) (2015).

[50] S. Greschner, M. Piraud, F. Heidrich-Meisner, I. P. McCulloch, U. Schollwöck, and T. Vekua, Spontaneous Increase of Magnetic Flux and Chiral-Current Reversal in Bosonic Ladders: Swimming against the Tide, Phys. Rev. Lett. **115**, 190402 (2015).

[51] B. Wang, X.-Y. Dong, F. N. Ünal, and A. Eckardt, Robust and ultrafast state preparation by ramping artificial gauge potentials, New J. Phys. **23** (2021).

[52] A. S. Sørensen, E. Demler, and M. D. Lukin, Fractional Quantum Hall States of Atoms in Optical Lattices, Phys. Rev. Lett. **94**, 086803 (2005).

[53] C. Repellin, J. Léonard, and N. Goldman, Fractional Chern insulators of few bosons in a box: Hall plateaus from center-of-mass drifts and density profiles, Phys. Rev. A **102**, 063316 (2020).

[54] B. Wang, X.-Y. Dong, and A. Eckardt, Measurable signatures of bosonic fractional Chern insulator states and their fractional excitations in a quantum-gas microscope, SciPost Phys. **12**, 95 (2022).

[55] J. Vidal, B. Douçot, R. Mosseri, and P. Butaud, Interaction Induced Delocalization for Two Particles in a Periodic Potential, Phys. Rev. Lett. **85**, 3906 (2000).

[56] M. Kremer, I. Petrides, E. Meyer, M. Heinrich, and O. Zilberberg, A square-root topological insulator with non-quantized indices realized with photonic Aharonov-Bohm cages, Nat. Commun. **11**, 907 (2020).

[57] B. M. Terhal, Quantum error correction for quantum memories, Rev. Mod. Phys. **87**, 307 (2015).

[58] J. M. Gertler, B. Baker, J. Li, S. Shiroi, J. Koch, and C. Wang, Protecting a bosonic qubit with autonomous quantum error correction, Nature (London) **590**, 243 (2021).

[59] Z. Liu, E. J. Bergholtz, and J. C. Budich, Dissipative preparation of fractional Chern insulators, Phys. Rev. Res. **3**, 043119 (2021).

[60] A. Eckardt, P. Hauke, P. Soltan-Panahi, C. Becker, K. Sengstock, and M. Lewenstein, Frustrated quantum antiferromagnetism with ultracold bosons in a triangular lattice, Europhys. Lett. **89**, 10010 (2010).